

# SCIENTIFIC AND TECHNICAL SECTION

UDC 539.4

## Effect of Cyclic Stresses below the Endurance Limit on the Fatigue Life of 40Cr Steel

L. H. Zhao,<sup>a,b,1</sup> J. Z. Feng,<sup>a,b</sup> and S. L. Zheng<sup>a,b</sup>

<sup>a</sup> School of Mechanical Engineering, University of Shanghai for Science and Technology, Shanghai, China

<sup>b</sup> CMIF Key Lab for Automotive Strength and Reliability Evaluation, Shanghai, China

<sup>1</sup> Pheigoe@126.com

*The effect of cyclic stresses below the endurance limit on the fatigue life of 40Cr medium-strength carbon steel is studied. Conventional constant-amplitude cyclic tests and specially designed variable-amplitude ones are conducted under torsional loading at the stress ratio  $R = 0.1$ . The results show that the strengthening effect of cyclic stresses below the endurance limit can be reached if they are applied prior to the exceeding ones. Moreover, the stress amplitude, number of cycles and load sequence are found to be the three major strengthening effect-controlling factors. Generally, different cyclic stress levels exhibit different strengthening effect values, whereas the respective fatigue strength will initially rise and then drop with the number of loading cycles. The cyclic stresses of a 85% endurance limit are established to provide the maximum strengthening effect. Under multi-level cyclic loadings, the strengthening effect at different cyclic stress levels is nonlinearly growing, and the total fatigue life is strongly related to the last level of stress amplitude in the load sequence. The scatter in fatigue lives is highly dependent on the loading conditions and strengthening effect. The coefficient of variance (COV) of fatigue life values exhibit the tendency to a decrease with the strengthening effect, which may improve the uniformity of the material fatigue strength characteristics.*

**Keywords:** variable amplitude load, strengthening effect, fatigue limit, load sequence effect, fatigue life.

**Introduction.** Fatigue fracture is the most common failure mode of engineering structures and components, whose fatigue life should be evaluated at the design stage to assure their safe and reliable long-term operation. Although many theories and models have been advanced for the fatigue strength and life assessment under variable-amplitude (VA) cyclic loads, the results obtained typically exhibit large discrepancies caused by the load sequence or load interaction effect [1].

Another source of such inconsistencies can be the overestimation of damage induced by cyclic stresses below the endurance limit. According to the existing fatigue models, all cyclic stresses in the VA loading schemes are assumed to be damaging [2]. However, some experimental results imply that the material fatigue strength can be improved by cyclic stresses below the endurance/fatigue limit, which increase the total fatigue life. Since the beginning of the last century, such terms as “strengthening effect” (SE) or “understressing effect” (UE) were applied to fatigue tests of ingot irons, Cr/Zn brass, and carbon steels [3, 4]. Moreover, multiple studies show that the SE of cyclic stresses below the endurance limit can be observed in many other materials, e.g., aluminum alloys [5, 6], metallic glasses [7],

fiber glasses [8], and carbon composites [9]. These results consistently indicate that the fatigue strength and life of materials can be considerably improved by SE, which should be taken into account in the fatigue strength assessment. However, to date, studies on the SE have been performed under simple loading conditions, such as understressing [5, 10], step incremental stress [7] or two-step repeated tests [4, 11], whereas only one level of stress amplitude below the endurance limit was considered. In practice, the mechanical structures and components are subjected to VA loading, which contain multi-level stresses below and above the endurance limit. Few studies have considered complex loading conditions, while most tests were conducted under tension–compression or bending loading conditions, while many load-bearing components are subjected to torsional loading. It is yet unknown whether the cyclic stresses below the endurance limit have any SE on the torsional fatigue life.

In this study, the effect of torsional cyclic stresses below the endurance limit on the fatigue strength and life is investigated for 40Cr medium-strength carbon steel, which is widely used in the driveshaft applications. Conventional fatigue tests under constant amplitude (CA) above the endurance limit and specific designs were performed. SE tests were conducted by applying three levels of load below the endurance limit for a certain number of cycles prior to the CA loading in the conventional fatigue tests. The results obtained are used to provide a more comprehensive understanding of the effect of cyclic stresses below the endurance limit on the fatigue life of carbon steels and are required for fatigue assessment of structures under the VA loading conditions.

**1. Experimental Details.**

**1.1. Material and Specimens.** The material tested in this study is 40Cr medium-strength carbon steel. The chemical composition of this material is presented in Table 1.

T a b l e 1

**Chemical Composition of the 40Cr Steel (wt.%)**

C	Si	Mn	Cr	Ni	Cu	P	S	Fe
0.37–0.44	0.17–0.37	0.5–0.8	0.8–1.1	≤ 0.03	≤ 0.03	0.035	≤ 0.035	Bal.

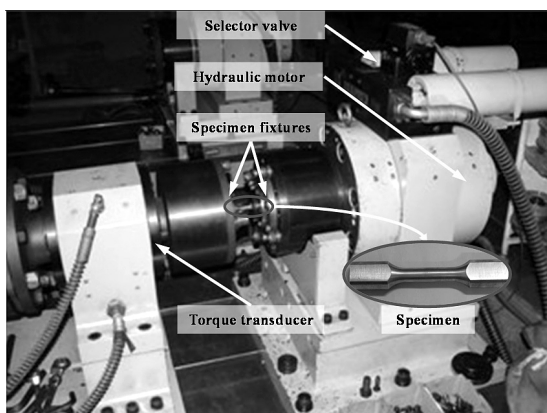


Fig. 1. Setup of the fatigue test.

The ultimate tensile strength (UTS), yield strength (YS) and elongation ( $\delta$ ) of the material are 980 MPa, 785 MPa, and 9%, respectively. The specimens are designed according to the China Standard GB 12443 (equivalent to ISO 1352) with a circular cross section having a radius of 6 mm. All specimens were tested under torsional conditions on a Saginomiya TT08 test machine (Fig. 1). The stress ratio  $R$  was set to 0.1. All specimens were tested at

30 Hz and room temperature in air. Prior to testing, the specimens were quenched at  $850 \pm 10^\circ\text{C}$ , tempered at  $520 \pm 10^\circ\text{C}$  and highly polished to diminish the effects of the surface roughness. At least three specimens were tested at each loading condition to cover the scatter of fatigue lives.

**1.2. Loading Conditions.** Considering the above SE-influencing factors, the fatigue tests are subdivided into three categories according to the aim and loading conditions: (1) conventional CA tests, (2) single-level SE tests, and (3) multi-level SE tests. The detailed information on each group is as follows:

**1.2.1. Conventional CA Tests.** The conventional CA tests are, in turn, subdivided into two groups. In the first group, the fatigue tests were conducted to determine the  $S-N$  curve and endurance limit. For the finite-life region, two specimens were tested at four different stress levels. The endurance limit was estimated using two specimens and the staircase method, and two other specimens were tested at two different levels to validate the derived  $S-N$  curve. In the second (reference) group, the fatigue tests were conducted at the stress amplitude of twice the endurance limit, to reduce the test time while assuring that the fatigue life falls into the high-cycle fatigue range. Eight specimens were tested to cover the scatter of fatigue life and guarantee the confidence level of the derived mean life.

**1.2.2. Single-Level SE Tests.** The single-level SE tests were conducted under a pre-understressing loading condition wherein the cyclic stresses below the endurance limit were applied prior to that above it. In this case, the specimens were first subjected to a strengthening load (below the endurance limit) for several cycles; then, they were tested under a damaging load or overload (above the endurance limit) until the final failure. The tests were subdivided into two groups. In the first group, the effect of the stress level on the SE was investigated. Under this condition, the strengthening load was set to 0.65, 0.75, 0.85, and 1.0 of the endurance limit, and the number of cycles was fixed at 200,000. The other group investigated the dependence between the numbers of cycles on the SE. The strengthening stress amplitude level was equal to 0.85 (i.e., 85%) of the endurance limit, and the number of cycles was set to 10,000, 50,000, 100,000, and 400,000. The loading conditions of single-level SE are illustrated in Fig. 2.

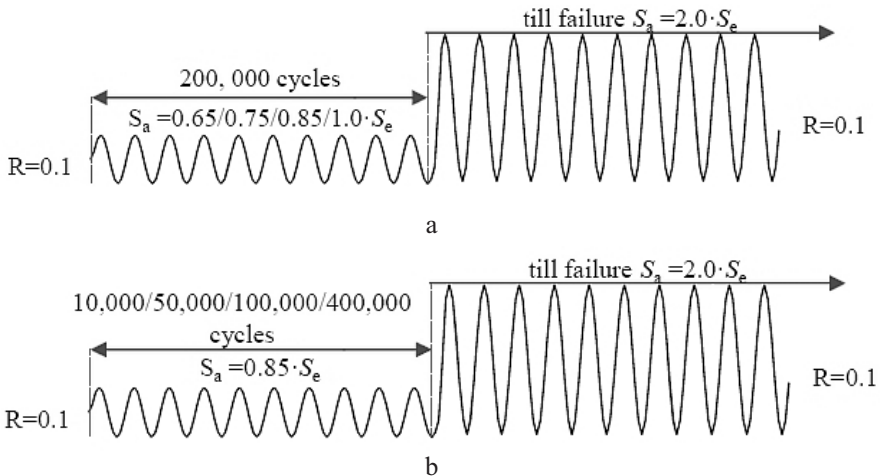


Fig. 2. Load conditions of single-level SE tests.

**1.2.3. Multi-Level SE Tests.** The multi-level SE tests were also conducted by pre-understressing, in order to investigate the integrated SE of multiple strengthening cyclic stress levels. The loading conditions are shown in Fig. 3. Here, three levels of cyclic stresses corresponding 0.65, 0.75, and 0.85 of the endurance limit  $S_e$ , respectively,

comprised each loading block. Three various loading blocks are adopted: (i) End@LA block ending with a low stress level equal to  $0.65S_e$ , (ii) End@MA block ending with a medium stress level of  $0.75S_e$ , and (iii) End@HA block with a high stress level of  $0.85S_e$ . The number of cycles of each stress level is set to 5500, 3500, and 1000, so that each loading block contains 10,000 cycles of cyclic stresses below the endurance limit. Specimens are subjected to 15 loading blocks before being tested at the stress amplitude twice exceeding the endurance limit until the final failure.

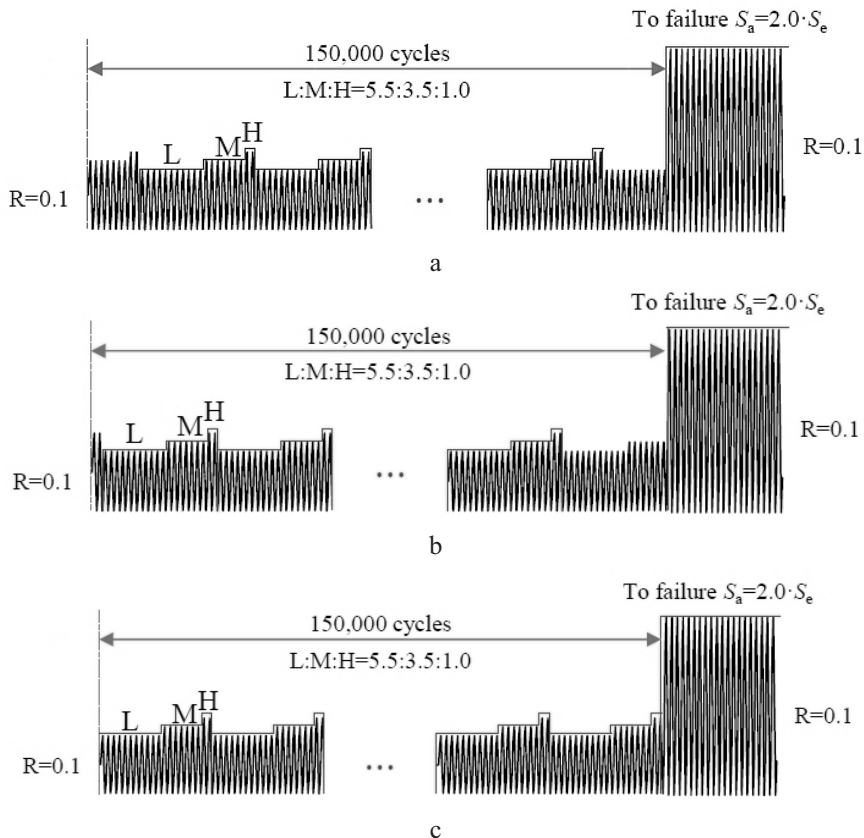


Fig. 3. Loading conditions of the multi-level SE tests. The stress amplitudes below the fatigue limit stop at different stress amplitudes: (a) End@LA; (b) End@MA; (c) End@HA.

**2. Results.**

**2.1. CA Test.** The conventional CA test results are depicted in Fig. 4. The median  $S-N$  curve for the finite-life range was constructed by regression analysis of the fatigue lives of eight specimens tested at four CA stress levels. The endurance limit was determined via two specimens tested under a smaller load level, which resulted in the fatigue lives exceeding  $10^7$  cycles. Two specimens (marked by +) were tested at higher and medium cyclic stress levels to validate the constructed/regressed  $S-N$  curve. Six specimens tested at the stress amplitude twice exceeding the endurance limit were used as the control group to validate the SE.

The regressed  $S-N$  curve has a close correlation with the test results, and all fatigue lives are within a scatter of two, as compared to the median  $S-N$  curve. However, the absolute scatter decreased with the stress level, which is consistent with the known trend of fatigue behavior. With the regressed  $S-N$  relation, the endurance limit corresponds to the stress amplitude of 277 MPa. Then, the cyclic stresses of 0.65, 0.75, 0.85, and 2.0 of the

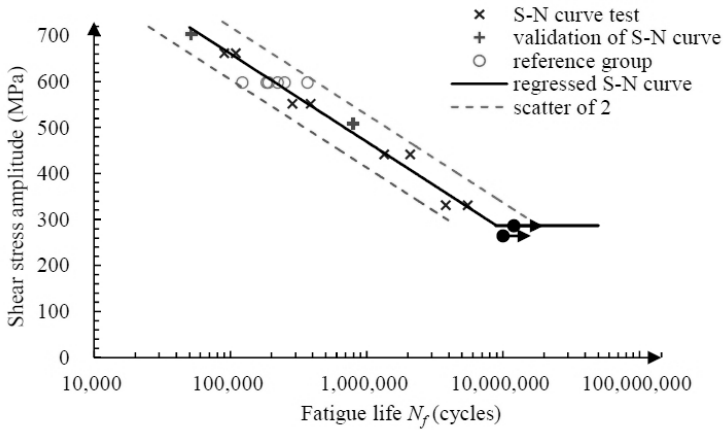
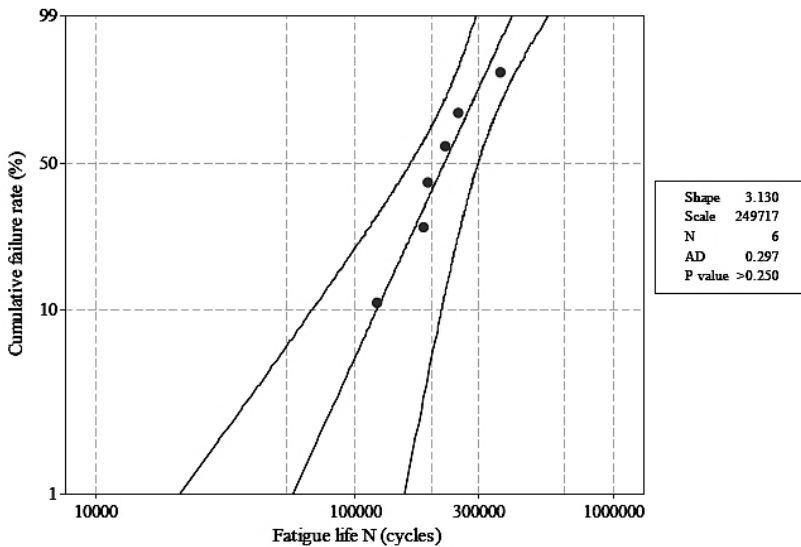
Fig. 4.  $S$ - $N$  curve and conventional CA tests.

Fig. 5. Fatigue life distribution of reference group.

endurance limit for the SE test were calculated. For the six specimens in the reference group (Fig. 5), the fatigue lives were 122,000–368,000 cycles with a mean value of 225,000 cycles.

**2.2. Single-Level SE Tests.** Figure 6 shows the fatigue lives of specimens strengthened by cyclic stresses at 0.65, 0.75, 0.85, and 0.95 of the endurance limit for 200,000 cycles. The resulting fatigue lives are consistent with the Weibull distribution. For the specimens strengthened by  $0.65S_e$ , the fatigue life was 277,000–489,000 cycles with a mean value of 389,000 cycles; for those strengthened by  $0.75S_e$ , the fatigue life was 365,000–586,000 cycles with a mean value of 541,000 cycles; and for those strengthened by  $0.85S_e$ , the fatigue life was 486,000–732,000 cycles with a mean value of 573,000 cycles. However, a decreasing tendency was observed when the stress amplitude was  $0.95S_e$ : the fatigue lives of the two specimens were 153,000 and 217,000 cycles, respectively.

The fatigue lives of specimens strengthened at  $0.86S_e$  for different numbers of cycles are shown in Fig. 7, which are also consistent with the Weibull distribution. For the specimens strengthened for 10,000, 50,000, 100,000, and 400,000 loading cycles the

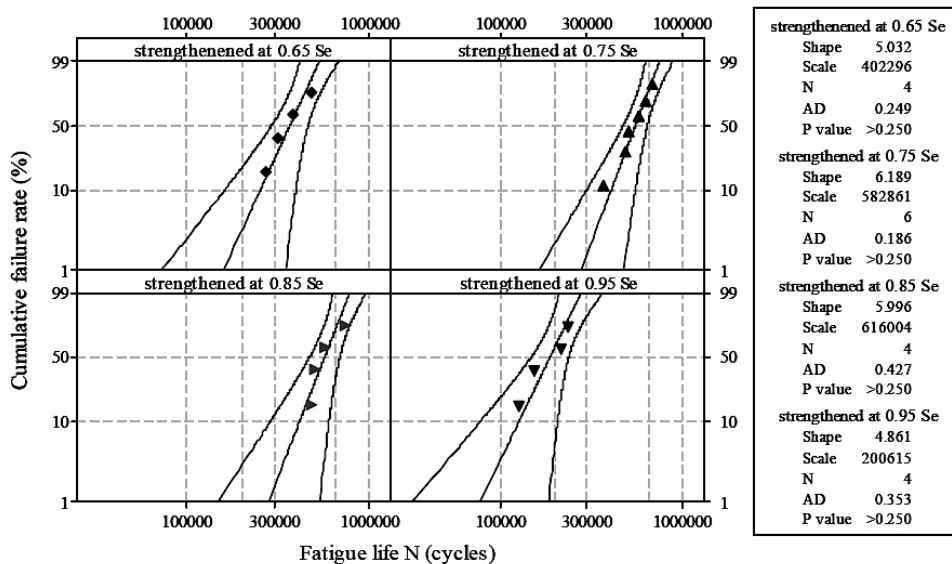


Fig. 6. Strengthening effects of different stress amplitudes below the fatigue limit.

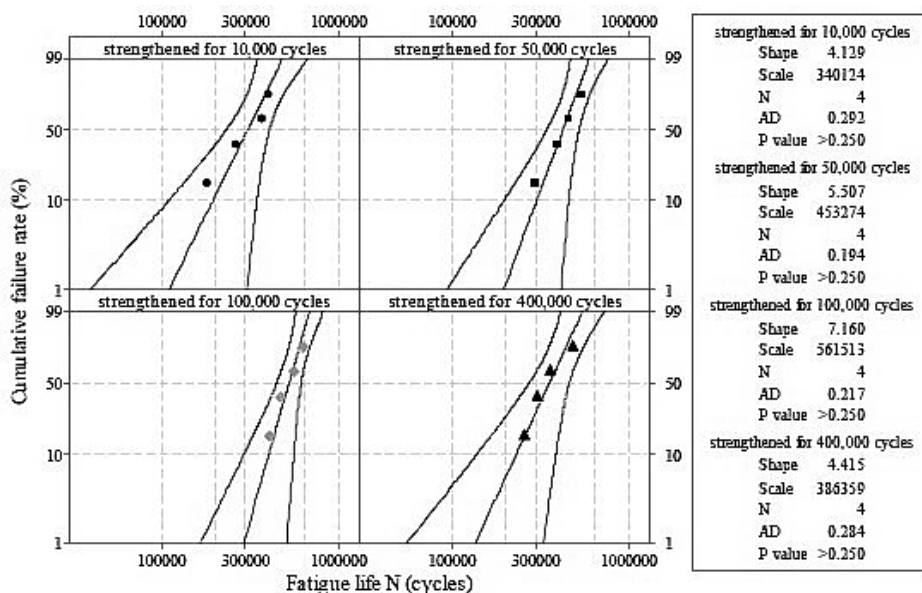


Fig. 7. Fatigue lives of specimens after strengthened at  $0.85S_e$  for different numbers of cycles.

respective fatigue lives were 182,000–371,000 cycles with a mean value of 310,000 cycles, 289,000–533,000 cycles with a mean value of 417,000 cycles, 416,000–638,000 cycles with a mean value of 525,000 cycles; and 258,000–486,000 cycles with a mean value of 352,000 cycles, respectively.

**2.3. Multi-Level SE Tests.** The results of the multi-level SE tests are shown in Fig. 8. For the specimens strengthened by the loading blocks ending with low stress amplitude (End@LA), the fatigue lives were 345,000–411,000 cycles with a mean value of 378,000 cycles. For those ending with a medium stress amplitude (End@MA), the fatigue lives were 297,000–352,000 cycles with a mean value of 332,000 cycles, while for those ending with

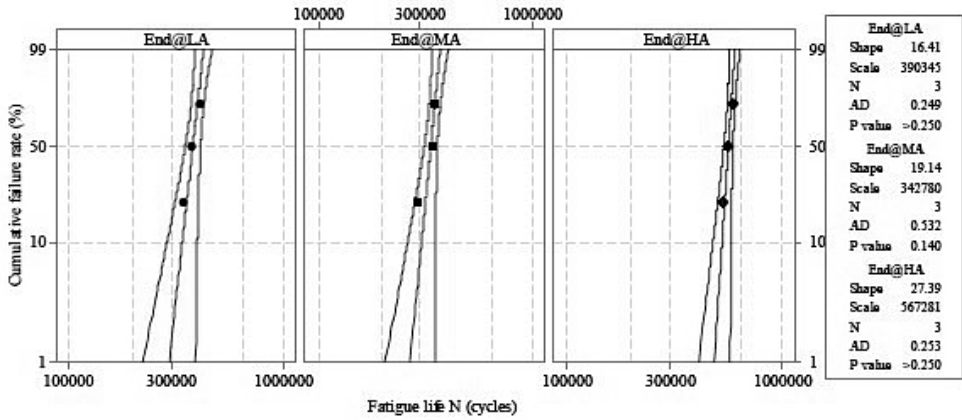


Fig. 8. Fatigue lives of specimens strengthened by multi-level strengthening stress amplitudes.

a high stress amplitude (End@HA), the fatigue lives were 527,000–585,000 cycles with a mean value of 556,000 cycles.

**3. Discussion.** The test results presented in Sect. 3 illustrate that the fatigue lives of all strengthened specimens were higher than those of specimens tested only under the stress amplitude above the endurance limit, except when the strengthening load was equal to  $0.95S_e$ . The changes in fatigue life and SE under different strengthening conditions are compared and quantitatively discussed below.

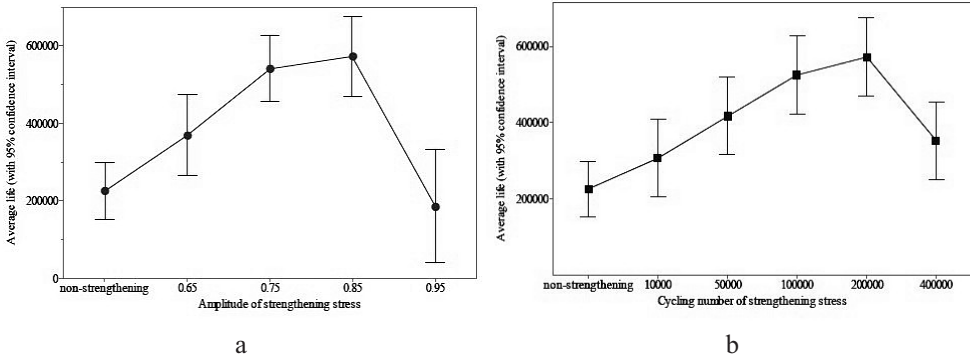


Fig. 9. Change in fatigue life under the single-level strengthening load condition: (a) the amplitude of the strengthening load varies; (b) the cycling number of strengthening loads varies.

Under single-level strengthening load conditions, the SE of the cyclic stresses below the endurance limit is highly correlated with the stress amplitude and number of cycles, as shown in Fig. 9. Firstly, different cyclic stresses below the endurance limit different effect on specimen total life. Cyclic stresses near the endurance limit ( $0.95S_e$  in this study) are of damaging effect, which finding was also reported elsewhere [12, 13], while the cyclic stresses below  $0.9S_e$  exhibit SE; and those of approximately  $0.85S_e$  provide the maximum SE. Secondly, the effect of the stress amplitude below the endurance limit on fatigue life depends on the number of cycles. During the first 200,000 cycles, the cyclic stresses below the endurance limit have a SE, whereas the following cycles have a damaging effect. This trend is identical to the observations in mild [14] and high strength steels [15] under bending loading conditions, although the transition points of the threshold number of cycles slightly differ in other material.

Under the multi-level loading conditions, the SE is also manifested but is highly correlated with the loading condition, as is shown in Fig. 10. Application of the End@HA loading blocks leads to the longest fatigue life, whereas the other two sequences have similar SEs. Insofar as the number of cycles for each stress level is considerably smaller than that in the single-level strengthening (where stress levels of 0.65, 0.75, and 0.85 $S_e$  correspond to 82,500, 52,500, and 15,000 cycles, respectively), this implies the SE accumulation under the multi-level loading conditions.

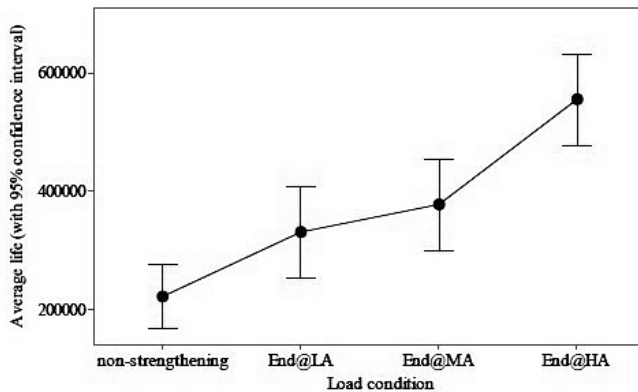


Fig. 10. Results of multi-level SE test.

The increase in fatigue life for the specimens strengthened by cyclic stresses means an improvement in the fatigue strength of the material. Based on the Basquin formula, the stress-life relation can be expressed as  $S_a^m N_f = C$ , where  $C$ ,  $S_a$ ,  $m$ , and  $N_f$  are the constants related to material, stress amplitude, fatigue strength exponent, and fatigue life, respectively. For the material under study, the fatigue life at stress level  $S_a$  was extended from  $N_f$  to  $N'_f$  by the SE of cyclic stresses below the endurance limit. Since a longer fatigue life  $N'_f$  corresponds to a smaller stress amplitude  $S'_a$ , the relative increment of fatigue strength  $\Delta S_a$  (%) can be calculated as follows:  $\Delta S_a$  (%) =  $(S_a - S'_a) / S_a \times 100\%$ .

Therefore, the fatigue strength of the tested 40Cr steel was improved by 7.59, 14.13, and 15.21% after application of 200,000 cycles of 3-level loading at the stress levels of 0.65, 0.75, and 0.85 $S_e$ , and by 4.68, 9.60, 13.61, and 6.82% after application of the preset number of cycles (described in Sect. 2.2) with the 0.85 $S_e$  stress level. From the approximate linear relation between SE and the number of cycles not exceeding 200,000 cycles, the fatigue strength enhancement caused by low, medium, and high cyclic stresses L (82,500 cycles), M (52,500 cycles), and H (15,000 cycles) in the multi-level SE tests is 3.13, 3.71, and 1.14%, respectively, with a total sum of 7.98% (Fig. 9b). This value is close to the fatigue strength increment of the End@LA (5.88%) and End@MA (7.95%) multi-level SE tests, but is lower than that of End@HA (14.65%). It confirms the nonlinear accumulation pattern of SE of different cyclic stress levels. Since the three loading block patterns have a similar loading sequence of L-M-H for the most period, the only difference between them are the stress levels, with which each loading block starts and ends. The total SE of multi-level strengthening tests is strongly related to the loading conditions, especially the last stress level, at which the strengthening treatment ends. Noteworthy is that the SE of multi-level cyclic stresses is studied only for a sequence of L-M-H, while other loading sequences H-M-L may result in different SE due to the load sequence effect [16, 17].

The fatigue life distributions under different loading conditions (Figs. 6–9) also indicate that the SE can considerably affect the fatigue life scatter. Figure 11 shows the relationship between the coefficient of variance of fatigue lives and the percentage increase

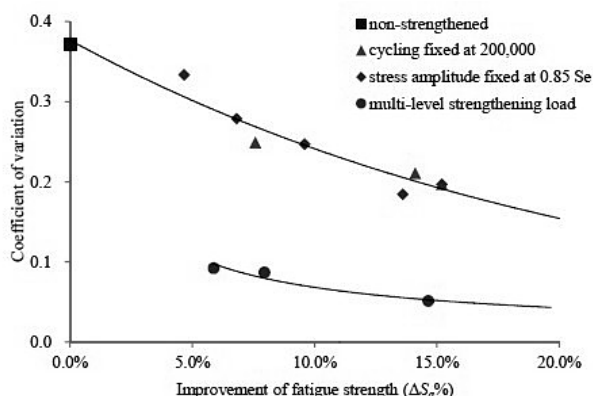


Fig. 11. Coefficient of variance vs SE.

in fatigue strength. The coefficient of variance tends to decrease with SE. This finding means that SE can improve the fatigue strength and uniformity of the material, particularly for specimens under multi-level strengthening loading conditions. In practice, structures are usually subjected to complex VA loading conditions including cyclic stresses below the endurance limit. The SE should be taken into account for fatigue durability assessments, in order to ensure the reliable design of structures and components subjected to cyclic loads.

**Conclusions.** This study experimentally investigates the SE of cyclic stresses below the endurance limit. Conventional fatigue tests and SE tests including three types of loading conditions (single- or multi-level SE tests and repeated block loading tests) were conducted on standard hourglass bar specimens. The main conclusions are as follows:

1. A significant SE can be observed for three types of loading conditions: single-level strengthening, multi-level strengthening and repeated block loading. For the investigated 40Cr steel, the mean fatigue life after coxing can increase by up to 2.5 times, this implies the respective fatigue strength improvement by more than 15%.

2. The SE is controlled by stress amplitude, number of cycles and sequences of the stress levels below the endurance limit. The maximum SE corresponds to the stress level of approximately 85% of the endurance limit. Under all investigated loading conditions, the SE initially increases and then decreases with the number of cycles of strengthening stress levels below the endurance limit.

3. Under multi-level strengthening conditions, a nonlinear accumulation of SE of different cyclic stress levels is observed. The total SE is strongly related to the load conditions, especially the last cyclic stress level of the strengthening treatment.

4. The SE controls the scatter of fatigue lives in the  $S-N$  curve. Under different strengthening conditions, the coefficient of variance of fatigue lives exhibits a decreasing tendency with SE, which implies that the later reduces the scatter in fatigue life experimental data.

**Acknowledgments.** This work was supported by the National Natural Science Foundation of China (Nos. 51375313 and 51705322), and SAIC Education Foundation Project (No. 1624).

1. J. Schijve, *Fatigue of Structures and Materials*, Springer Netherlands (2001).
2. J. Lemaitre and R. Desmorat, *Engineering Damage Mechanics: Ductile, Creep, Fatigue and Brittle Failures*, Springer-Verlag, Berlin–Heidelberg (2005).
3. G. Sinclair, *An Investigation of the Coxing Effect in Fatigue of Metals*, Illinois University at Urbana (1952).

4. S. Teimourimanesh and F. Nilsson, "Effects of cycles below the fatigue limit on the life of a high strength steel," *J. Test. Eval.*, **37**, No. 3, 201–204 (2009).
5. L. Zeng, Z. Li, R. Che, et al., "Mesoscopic analysis of fatigue strength property of a modified 2618 aluminum alloy," *Int. J. Fatigue*, **59**, 215–223 (2014).
6. Y. Takahashi, H. Yoshitake, R. Nakamichi, et al., "Fatigue limit investigation of 6061-T6 aluminum alloy in giga-cycle regime," *Mater. Sci. Eng. A*, **614**, 243–249 (2014).
7. A. B. El-Shabasy and J. J. Lewandowski, "Fatigue coaxing experiments on a Zr-based bulk-metallic glass," *Scripta Mater.*, **62**, No. 7, 481–484 (2010).
8. M. Tomozawa, P. Lezzi, R. Hepburn, et al., "Surface stress relaxation and resulting residual stress in glass fibers: A new mechanical strengthening mechanism of glasses," *J. Non-Cryst. Solids*, **358**, Nos. 18–19, 2650–2662 (2012).
9. Y. Tanabe, T. Yoshimura, T. Watanabe, et al., "Fatigue of C/C composites in bending and in shear modes," *Carbon*, **42**, Nos. 8–9, 1665–1670 (2004).
10. X. Lu and S. L. Zheng, "Strengthening and damaging under low-amplitude loads below the fatigue limit," *Int. J. Fatigue*, **31**, No. 2, 341–345 (2009).
11. L. Zhao, S. Zheng, and J. Feng, "Fatigue life prediction under service load considering strengthening effect of loads below fatigue limit," *Chin. J. Mech. Eng.*, **27**, No. 6, 1178–1185 (2014).
12. A. Singh, "The nature of initiation and propagation  $S-N$  curves at and below the fatigue limit," *Fatigue Fract. Eng. Mater. Struct.*, **25**, No. 1, 79–89 (2002).
13. C. Fukuoka and Y. G. Nakagawa, "Microstructural evaluation of cumulative fatigue damage below the fatigue limit," *Scripta Mater.*, **34**, No. 9, 1497–1502 (1996).
14. S. L. Zheng and X. Lu, "Microscopic mechanism of strengthening under low-amplitude loads below the fatigue limit," *J. Mater. Eng. Perform.*, **21**, No. 7, 1526–1533 (2012).
15. X. Lu and S. L. Zheng, "Strengthening of transmission gear under low-amplitude loads," *Mater. Sci. Eng. A*, **488**, Nos. 1–2, 55–63 (2008).
16. M. Vormwald, "Classification of load sequence effects in metallic structures," *Procedia Engineer.*, **101**, 534–542 (2015).
17. M. Gladskyi and A. Fatemi, "Load sequence effects on fatigue crack growth in notched tubular specimens subjected to axial and torsion loadings," *Theor. Appl. Fract. Mech.*, **69**, 63–70 (2014).

Received 15. 09. 2017